THE EFFECT OF WATER VAPOUR TRANSFER ON NATURAL CONVECTION IN BUILDING CAVITIES

D.J. Close, H. Suehrcke and A. Masatto
Department of Mechanical Engineering
James Cook University
Townsville 4811, Australia

ABSTRACT

Previous work has shown that for saturated air/water vapour mixtures, water vapour transfer in cavities can cause very large increases in net energy transfer due to its effect on natural convection. Given that many materials used in building envelopes adsorb water vapour, then in many situations a water vapour pressure gradient will exist across a cavity, leading to water vapour transfer across the cavity. In these situations the mixture is generally not saturated but some effect of the water vapour transfer on natural convection can be expected.

This paper lists the dimensionless groups that are expected to influence natural convection in unsaturated air/water vapour mixtures. It then describes experiments used to determine energy transfer rates in cavities bounded by horizontal isothermal surfaces, the lower and hotter of which was covered with a saturated aqueous salt solution generating a vapour pressure less than that of saturated water. The upper and cooler metal surface only exerted a vapour pressure when conditions were such that condensation occurred on it.

Results from the experiments show increases of up to three times in convective energy transfer when condensation occurred, as compared to cases where no mass transfer occurred, even when only modest vapour pressures were generated by the heated salt solution. The magnitude of the results supports the postulate of natural convection enhanced by mass transfer occurring in such cavities, and in many real situations will need to be included in building thermal load calculations.

1. INTRODUCTION

Moisture transfer in building elements can be significant in the overall thermal response of buildings. Coupled heat and mass diffusion has been demonstrated to play a role in small and simple structures [1], although the effect is influenced by the building design, materials used and climate.

Presently, energy transfer through cavities in the building envelope is based on heat transfer only in air and data from ASHRAE [2] usually forms the basis for heat transfer calculations. However, many common building materials adsorb water and consequently exert vapour pressures between zero and that of water at the temperature of the material surface. Saturation water contents for various common building materials are shown in Table 1 below. If a cavity exists in a wall, where the materials on either side of the cavity are for example concrete brick and plaster board, then the possibility for water vapour transfer across the cavity exists.

An estimate of the maximum effect to be expected can be obtained from the case where the water vapour pressures on the surfaces of the cavity correspond to saturation conditions. A theory for this situation was developed by Close and Sheridan [6], and verified experimentally by Close and co-workers [7], and the theory allows the effective Nusselt number and hence effective heat transfer coefficient to be calculated.

Assume that a vertical cavity, 90mm wide and infinite in extent in the other two dimensions, has isothermal surfaces on either side of the cavity. The isothermal surfaces are assumed to be covered with water so that the vapour pressures correspond to a free water surface. The data from ASHRAE [2] gives a convective conductance across the cavity of 1.44 $W/m^2 \cdot K$ for air, whereas the case with the isothermal surfaces covered with water gives an effective conductance of 8.90 $W/m^2 \cdot K$, using the procedure developed in [6].

Of course the case discussed above is an extreme one, and one would expect the real situation to lie somewhere between it and the heat transfer only case. The psychrometric chart in Fig. 1 helps to clarify the situation, with air states in equilibrium with the surfaces, characterising the cavity walls. The wall temperatures, one hot and one cold are maintained constant as is the equilibrium absolute humidity of the cold surface. If the equilibrium absolute humidity of the hot surface is below that of the cold then one would expect vapour to flow from cold to hot surface in opposition to the direction of heat flow, so reducing the total energy flow below that for heat transfer only. If the two absolute humidities are equal then one would expect no vapour flow, and the energy flow to be equal to the heat transfer only. When the absolute humidity of the hot surface is higher than that corresponding to the cold surface, then vapour flows from the hot to

cold surface so that the energy flow is higher than that due to heat transfer alone.

The absolute humidities of the hot and cold surfaces result from the properties of the materials and the history of the envelope, which is in turn driven by the ambient and building internal temperatures. This illustrates the necessity for incorporating the effect of water vapour transfer into building simulation codes.

2. EXPERIMENTAL AND THEORETICAL PROGRAM

In dealing with natural convection in enclosures with saturated gas/vapour mixtures, the equations for the coupled heat and mass transfer case were recast in a form exactly the same as those for heat transfer alone in a single component fluid, [6]. With modified Nusselt, Grashof and Prandtl numbers based on mixture properties, the similarity in the equation sets allowed existing functional relationships for heat transfer to be used to calculate effective heat transfer coefficients for the coupled heat and mass transfer case. Obviously a similar strategy for the unsaturated mixture would be a most attractive option. However, the dependence of the partial pressure of the vapour component on the water contents and temperatures of the bounding surfaces suggests that transforming the equations from ones with temperature and humidity as property variables to ones with a single variable such as temperature, is an unlikely outcome.

An alternative approach has been to transform the equation set using combined potentials of the form

$$F = T \pm c\,m$$

This method, first proposed by Henry [8], has been used in a range of coupled heat and mass transfer cases. Unfortunately, no such potentials have been found allowing the equations to be written in terms of them.

Hence, the approach used has been to obtain experimental data and then correlate the data in terms of the dimensionless groups derived from the governing heat, mass, momentum and continuity equations and the associated boundary conditions.

The groups obtained in this way are

$$A = L/H$$

$$Re = \rho_m L\, u_\infty / \mu_m$$

$$Gr = g\beta_T \Delta T L^3 / \nu_m^2$$

$$Pr = \frac{1}{1+m}(\partial h_m / \partial T)\, \mu_m / k_m$$

$$Sc = \nu_m / D$$

with additional parameters

$$P_1 = \beta_T \Delta T / \beta_m \Delta m \quad \text{buoyancy force ratio;}$$

$$P_2 = \frac{\rho_d D\, h_{fg} \Delta m}{k_m \Delta T} \quad \text{ratio of energy transfer rate due to mass transfer, to heat transfer rate;}$$

and from the boundary conditions,

$$Nu = h_c L / k_m$$

$$Sh = h_D L / \rho_m D$$

The remainder of the paper describes preliminary experiments and the results obtained from them.

3. EXPERIMENTAL APPARATUS AND METHOD

3.1. APPARATUS

The heat transfer measurements were carried out in a rectangular cavity (square in cross section) where the cavity consists of four insulated vertical walls closed off by two isothermal horizontal plates. Fig. 2 shows a layout of the experimental apparatus.

The lower horizontal composite plate consists of an electrically heated plate placed flat on top of a water heated plate with four heat flux meters between the two. The upper horizontal plate is similar but electrical heating was not used, and it was connected to the mains water supply while the lower (hotter) plate was connected to a temperature controlled water bath. Power supplied to the lower plate was adjusted to null the heat flux meter readings, so that all this power passed from the plate into the cavity.

The horizontal aluminium plates were designed to keep the temperature difference across the plate to less than 0.1 K at maximum power supply output. Five copper-constantan thermocouples were placed in each set of plates and connected in series to give an average plate temperature. All thermocouple connections were referenced to an ice-bath and the resulting thermocouple output voltages were measured with a precision voltmeter. The heat flux meters were connected in series to give an average heat flux across the electrically heated plate. The vertical walls were constructed using polystyrene insulation 50 mm thick, and the inner surfaces were covered with 0.8 mm steel linings to provide water vapour barriers.

3.2. EXPERIMENTAL METHOD

The temperature differences between the lower hot plate and the upper cold plate were used to set up water vapour concentration differences between the lower and upper plates using saturated aqueous salt solutions of either LiCl or $MgCl_2$ in a shallow stainless steel dish on top of the electrically heated lower plate. This arrangement maintained the water vapour pressure below the saturation value at the lower plate (relative humidities approximately 0.11 and 0.31 for LiCl and $MgCl_2$ respectively [9]).

The heat transfer experiments were carried out for four plate spacings (125, 250, 375, 500 mm) and four hot plate temperatures (40, 50, 60, 70°C) for both LiCl and $MgCl_2$. In addition heat transfer measurements with the stainless steel dish empty were carried out for 125 mm plate spacing at hot plate temperatures of 50, 60, 70 and 80°C. The cold plate temperature was approximately 26°C for all measurements. Steady state conditions were considered to be achieved when the deviation of the heat flux meter readings about zero was less than + or -5% of the supplied power, maintained for no less than 30 minutes.

The aim of the experiment was to find the net convective energy transfer between the hot and cold plates. However, the measurements of heat flow from the bottom plate also included side wall losses and the effects of heat conduction and thermal radiation heat transfer between upper and lower plates. In order to remove these effects the following procedures were adopted.

For the heat transfer measurements with the stainless steel dish empty (no liquid surface), the effects of side wall losses, conduction between the plates via the steel side walls, and thermal radiation heat transfer between them were removed by calibrating the apparatus in the inverted position (cavity heated from above). It was assumed that in the inverted position heat transfer through the cavity was by conduction only. As the case for conduction can be calculated, comparisons were made between the theoretical and experimental heat transfer values, with the differences being the side wall losses and the conduction and thermal radiation heat transfer between plates. The side wall losses and conduction and radiation heat transfers determined in this manner were subtracted from each measurement of input power to obtain the net heat transfer due to convection. The method is justified by the good agreement between the corrected measurements and the relationship

$$Nu = 1 + 0.0585\ Ra^{1/3}$$

derived from Hollands [10], and shown in Fig 3.

For the heat transfer measurements involving the saturated aqueous salt solutions of LiCl and $MgCl_2$, the above data correction could not be used as the introduction of a liquid surface at the bottom plate changes the surface emissivity and therefore the radiative heat transfer. Moreover, the emissivity of the top plate changes when condensation on it occurs. However, a measurement of the emissivity of the heavily corroded top aluminium plate suggested that the change in its emissivity due to condensation would be small. For this reason the measurements involving LiCl, and $MgCl_2$ when no condensation occurred, were corrected so that they agreed with the relationship of Hollands,[10], and this correction was then applied to those $MgCl_2$ cases where condensation did occur. It was assumed that the condensate droplets falling back into the salt solution did not significantly influence the heat transfer.

4. RESULTS AND CONCLUSIONS

The experimental results, compared with air only predictions from Hollands [10] and with predictions for saturated mixtures using the similarity theory of Close and Sheridan [6], are given in Fig.3.

As shown, the corrected results for the LiCl solution experiment are in line with the air only calculations. While corrections were applied to ensure this, it is important to note that the gradients for the two sets of numbers are very close, reinforcing the validity of the LiCl data. Given the low humidities generated by the saturated LiCl solution so that no condensation occurred on the cold plate, these results should agree with predictions for air only using Hollands' correlation.

The results for the $MgCl_2$ solution show the effect of transferring water vapour from the hot to the cold plate. At low temperatures there is little or no effect with the $MgCl_2$ data coinciding with those from the LiCl experiment. As the solution temperature is increased so the vapour pressure generated by the solution increases and mass transfer occurs. For each of the cavity heights, increases in the hot plate temperature result in an increase in the ratio of the Nusselt number for the mass transfer case to that for air only, reflecting the increase in P_2 as the ratio of concentration difference to temperature difference increases. If a salt with a higher vapour pressure at a given temperature than $MgCl_2$ was used then one would expect a higher ratio. In the limit, Nusselt numbers corresponding to the saturation case would be expected.

Obviously, considerably more data is required to correlate the results with the large number of parameters. However, it is clear that significantly higher cavity conductances can occur than are given by heat transfer only correlations.

During the course of the experimental program, significant difficulties were encountered in the corrections required due to radiation transfer, side wall losses and conduction up the walls. Future experiments must take account of these effects, as well as tackling the problem of setting the cold plate equilibrium absolute humidity at less than saturation, and having vertical rather than horizontal heated and cooled plates.

Finally it was decided that insufficient data existed to attempt a general correlation of Nu vs the five significant parameters. The parameter list excludes Re and assumes that Ra is formed from the product of Gr and Pr.

ACKNOWLEDGMENTS

The authors wish to acknowledge the considerable assistance and advice from Mr John Findlay of the Department of Mechanical Engineering, James Cook University, and thanks the CSIRO Division of Building, Construction and Engineering for the loan of the apparatus used to conduct the experiments.

REFERENCES

1. A.Delsante, J.G.Symons, J.W.Clarke, J.W.Spencer, J.V.Peirce, D.J.Close and D.Hosking, The Thermal Performance of Wool Insulation in Transportable Buildings. CSIRO Division of Building, Construction and Engineering, Report DBCE Doc. 92/147, December 1992.

2. American Society of Heating, Refrigeration and Air-Conditioning Engineers, Fundamentals Handbook. ASHRAE, Atlanta, 1993.

3. Paul Marsh, Air and Rain Penetration of Buildings. The Construction Press Ltd, Lancaster, 1977.

4. K.K.Kelley, J.C Southard and C.T.Anderson, Thermodynamic Properties of Gypsum and its Dehydration Products. United States Department of the Interior, Bureau of Mines, Technical paper 625, 1941.

5. Ralph M. Nelson Jnr, A Model for Sorption of Water Vapour by Cellulosic Materials. Wood and Fibre Science, 15(1), 1983.

6. D.J.Close and J. Sheridan, Natural Convection in Enclosures Filled with a Vapour and a Non-Condensing Gas. Int.J.Heat Mass Transfer, 32(5), 1989.

7. D.J.Close, M.K.Peck, R.F.White and K.J.Mahoney, Buoyancy Driven Heat Transfer and Flow Between a Wetted Heat Source and an Isothermal Cube. J.Heat Transfer, 113(2), 1991.

8. P.S.H. Henry, Diffusion in Absorbing Medium. Proc R. Soc., Ser. A, 171, 1939

9. D.T. Acheson, Humidity and Moisture Vol. 3 (ed. A. Wexler), pp 521-530, Reinhold 1965.

10. K.G.T. Hollands, Natural Convection in Horizontal Thin-Walled Honeycomb Panels, ASME Publication 72-HT-60, 1972.

NOMENCLATURE

A	-	L/H - aspect ratio	[-]
c	-	constant	[K^{-1}]
D	-	mass diffusivity	[m^2/s]
F	-	$T \pm c\,m$ - combined potential	[K]
g	-	gravitational acceleration	[m/s^2]
H	-	cavity dimension	[m]
h_c	-	convective heat transfer coefficient	[$W/m^2.K$]
h_D	-	convective mass transfer coefficient	[$kg/m^2.s$]
h_{fg}	-	latent heat of vaporisation	[J/kg]
h_m	-	enthalpy of air/water vapour mixture	[J/kg]
k_m	-	thermal conductivity of water vapour mixture	[W/m.K]
L	-	cavity dimension	[m]

m	-	absolute humidity	[-]
Nu	-	Nusselt number	[-]
Ra	-	Rayleigh number	[-]
Re	-	Reynolds number	[-]
T	-	temperature	[K]
u	-	velocity	[m/s]
β_m	-	buoyancy due to concentration gradients	[-]
β_T	-	buoyancy due to temperature gradients	[K^{-1}]
Δm	-	absolute humidity potential	[-]
Sh	-	Sherwood number	[-]
ΔT	-	temperature potential	[K]
ρ_d	-	density of air in air/water vapour mixture	[kg/m^3]
ρ_m	-	density of mixture	[kg/m^3]
ν_m	-	kinematic viscosity of mixture	[m^2/s]
μ_m	-	dynamic viscosity of mixture	[$N.s/m^2$]
Sc	-	Schmidt number	[-]
Pr	-	Prandtl number	[-]
P_1, P_2	-	parameter groups defined in text	[-]

Table 1
Saturation Water contents of Some Common Building Materials

Material	Saturation Water Content % Dry Weight	Ref
Stone	0.1 - 11.6	[3]
Bricks	4.5 - 24	[3]
Concrete	6.7 - 15	[3]
Wood	30	[4]
Gypsum Plaster	21	[5]

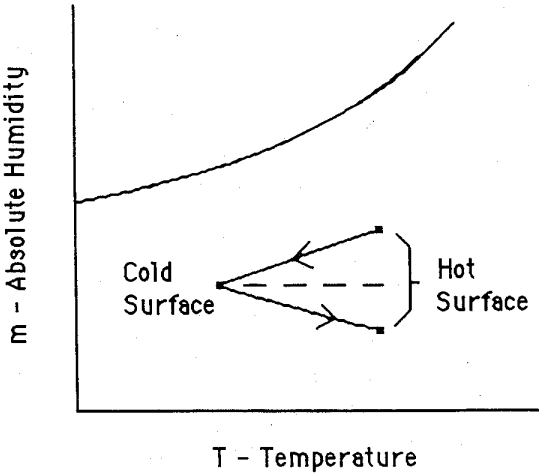

Fig.1. Psychrometric sketch illustrating vapour flows, shown by arrows for different hot and cold surface states.

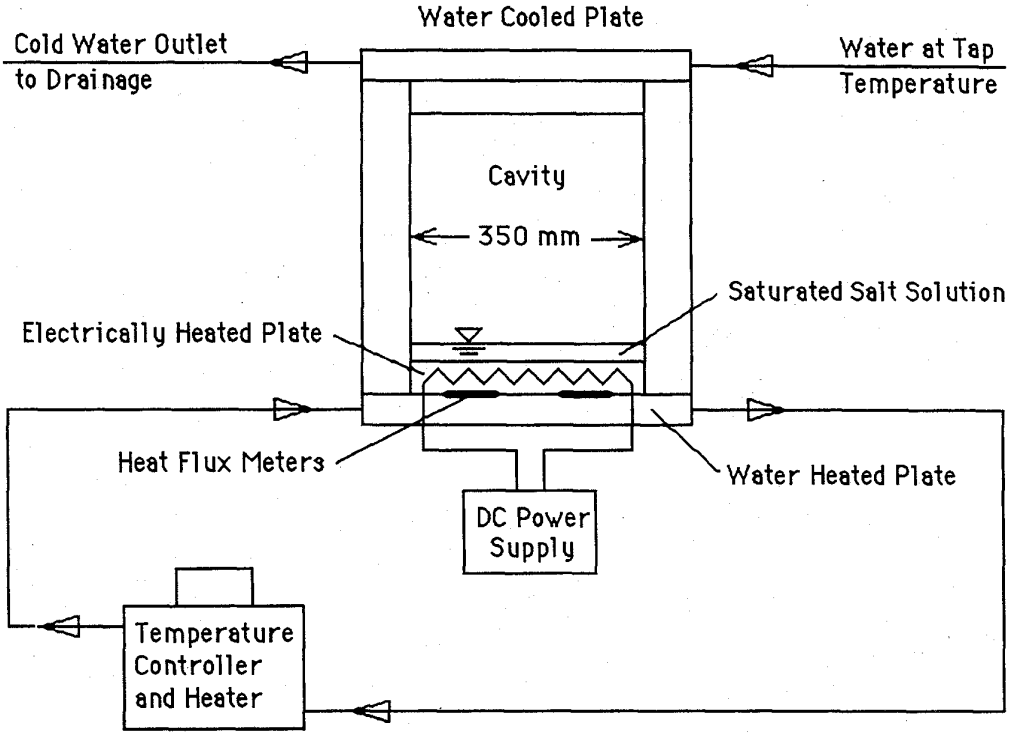

Fig. 2. Schematic Diagram of Experimental Apparatus.

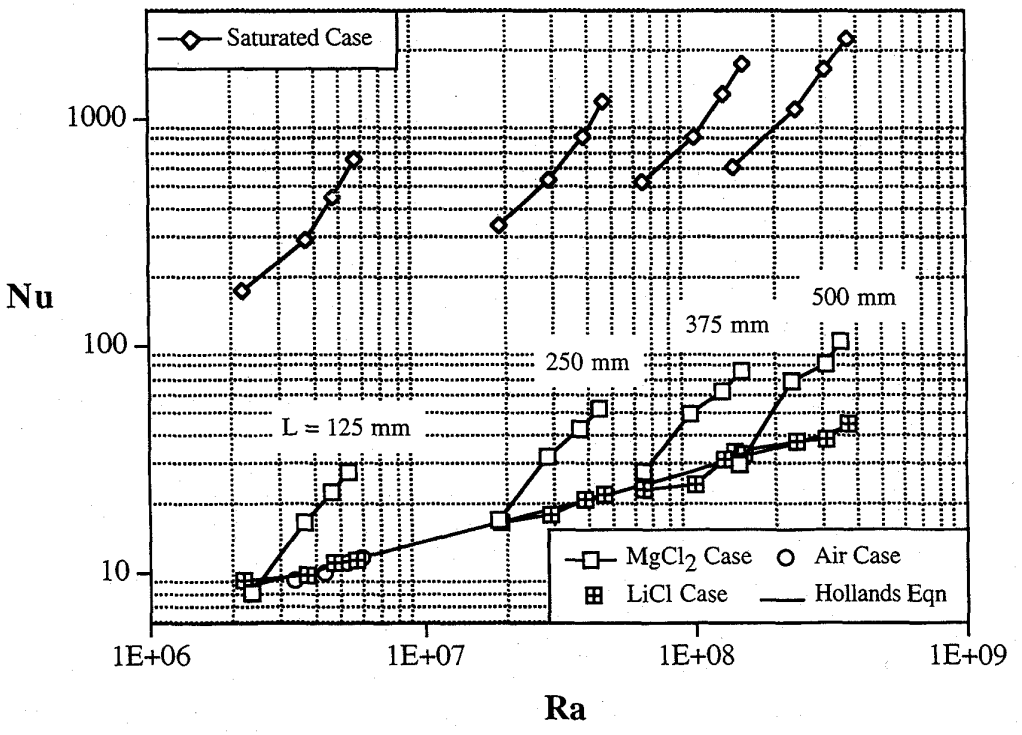

Fig. 3. Comparison of the experimental results with energy flows for the saturated and the air only case.